Weak ferromagnetism in Mn nanochains on the CuN surface

A. N. Rudenko,[1,2] V. V. Mazurenko,[1,2] V. I. Anisimov,[1,3] and A. I. Lichtenstein[2]
[1]*Department of Theoretical Physics and Applied Mathematics, Urals State Technical University, Mira Street 19, 620002 Ekaterinburg, Russia*
[2]*Institute of Theoretical Physics, University of Hamburg, Jungiusstrasse 9, 20355 Hamburg, Germany*
[3]*Institute of Metal Physics, Russian Academy of Sciences, 620219 Ekaterinburg GSP-170, Russia*
(Received 23 December 2008; revised manuscript received 11 March 2009; published 15 April 2009)

We investigate the electronic and magnetic structures of Mn chains supported on a CuN surface, using first-principles LSDA and LDA+U methods. The isotropic exchange integrals and anisotropic Dzyaloshinskii-Moriya interactions between Mn atoms are calculated using the Green's function technique and total energies difference method. It is shown that lattice relaxation and on-site Coulomb interaction are important for an accurate description of the magnetic properties of the investigated nanosystems. Based on a classical spin Hamiltonian we conclude that the Mn antiferromagnetic nanochains on the CuN surface demonstrate weak ferromagnetism. The net magnetic moment and direction of the spin canting are estimated in the framework of a classical spin Hamiltonian. We show that some aspects of the experimental spectrum can be explained using a quantum spin Hamiltonian, with parameters defined from first-principles calculations and extracted from recent STM experiments.

DOI: 10.1103/PhysRevB.79.144418 PACS number(s): 73.22.−f, 75.30.Et

I. INTRODUCTION

The investigation of magnetic nanomaterials is an important part of modern nanoscience that exerts influence on progress in different sectors of technology (for instance, medicine devices for therapy and diagnostics,[1,2] magnetic data storage systems,[3] etc). Using intrinsic magnetic moments scientists can change physical properties of nanomaterials by applying external magnetic field. The technological applications of magnetic nanomaterials should base on an accurate control of the coupling between individual spins.

Recently, Hirjibehedin *et al.*[4] have reported the fabrication of Mn nanoparticles in the form of linear chains that display a truly collective quantum behavior. Using local spin-excitation spectroscopy technique, based on inelastic scanning tunneling microscopy (STM), they were able to show how the quantum properties of this system depend on the number of atoms involved. They demonstrated a unique method to measure and to control the magnetic interactions between Mn atoms. The experimental spectra were analyzed by authors using the simplest form of the Heisenberg model with exchange interactions between the nearest neighbors. However, there are some aspects of the Mn chain spectra that are not understood in the framework of the Heisenberg model: (i) a zero-field splitting that grows in energy with increasing chain length, (ii) different zero-field energies of the $m=\pm 1$ and $m=0$ excited states and (iii) an asymmetry of the spectra with respect to voltage polarity.

Jones and Lin[5] have applied GGA+U approach to describe the electronic and magnetic structures of single and pair of Mn atoms on the CuN(100) surface. The performed spin-density analysis shows that Mn atoms on such surface preserve their atomic spins $S=\frac{5}{2}$. This result agrees with STM measurement.[4] Electron-density change and surface relaxation due to Mn atoms were also analyzed in Ref. 5.

The combination of an experimental STM approach and a theoretical *ab initio* method[6] has been used to describe the large magnetic anisotropy of individual Mn and Fe atoms on the CuN surface. The authors of Ref. 6 have provided the phenomenological picture of the magnetic anisotropy. For that purpose, the experimental spectra at different magnetic fields were fitted with a simple on-site spin Hamiltonian. Based on the fitting results they concluded that in case of manganese system the easy axis is oriented out of plane.

In this paper we show that the local distortion of the system results in superexchange isotropic interactions between Mn atoms through 2p orbitals of N atoms. These interactions are calculated using the Green's function approach and total energies difference method. Having diagonalized the Heisenberg Hamiltonian we estimate the energies of the first magnetic excitations. The obtained results are in good agreement with experimental data.

In the previous theoretical investigations noncollinear magnetic ground states for nanostructures on nonmagnetic and magnetic surfaces were proposed.[7–9] For instance, the calculations results for the noncollinear triangular compact trimer of Cr on the Au(111) (Ref. 7) predict that the angle between each pair of Cr moments equals to 120° and, therefore, the total spin moment is zero. In this case the noncollinearity is the result of frustration of the trimer magnetic interactions.

In the paper[8] authors have investigated different structures of Fe, Mn, and Cr atoms on the Cu(111) surface. The Fe clusters were found to be ferromagnetically ordered. Whereas for the Mn and Cr clusters the antiferromagnetic exchange interactions between nearest neighbors have been found. The antiferromagnetic couplings produce either collinear or noncollinear magnetic structures due to frustration of cluster geometry.

Interesting results for the trimer and tetramer configurations of Mn and Cr atoms on the magnetic Ni(111) surface were obtained in the paper.[9] One should stress that there are two types of a magnetic frustration: (i) frustration within adcluster and (ii) frustration arising from competing magnetic interactions between adclusters and surface atoms.

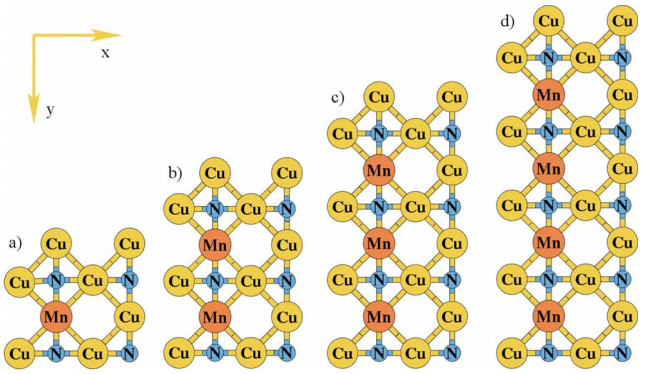

FIG. 1. (Color online) Structure of supercells containing $Mn_n(n=1\ldots4)$ chains on the CuN(100) surface (top view).

Another source of the noncollinearity was proposed in Ref. 10. Spin-polarized scanning tunneling microscopy experiments have shown that manganese spins on a tungsten (110) substrate are slightly canted antiferromagnetic. The resulting magnetic structure is a spin spiral the authors interpreted using Dzyaloshinskii-Moriya interaction.

We found the same mechanism of the spin noncollinearity for Mn dimer on the CuN surface. According to our calculations a local distortion between Mn atoms in the nanochain results in the strong Dzyaloshinskii-Moriya (DM) interaction. An important role plays a displacement of N atom out of the surface. Based on first-principles calculations of the Dzyaloshinskii-Moriya interactions between magnetic moments we point out that the Mn nanochains on the CuN demonstrate weak ferromagnetism. This result is also confirmed by direct LDA+U+SO calculations. Some aspects of experimental spectra can be reproduced with a quantum spin Hamiltonian that contains single-ion anisotropy, isotropic and anisotropic exchange interactions.

The rest of the paper is organized as follows. In Sec. II we describe the methods of the investigation. In Secs. III A and III B we present the results of local spin-density approximation (LSDA) and LDA+U calculations, respectively. The analysis and comparison of obtained exchange interactions with experimental data are given in Sec. III C. The discussion of Dzyaloshinskii-Moriya interactions in investigated systems is presented in Sec. III D. Section IV is devoted to the analysis of zero-field energy splitting observed in STM experiment and in Sec. V we briefly summarize our results.

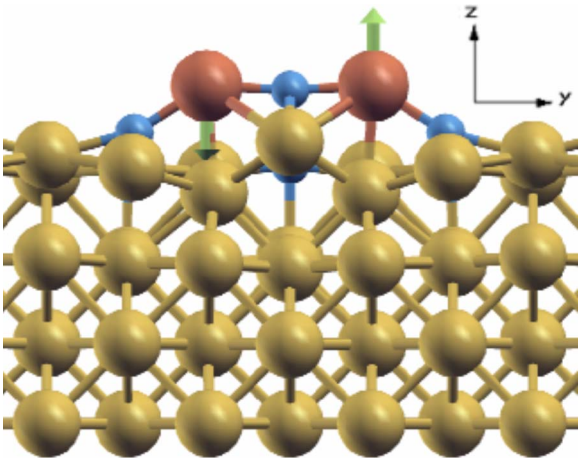

FIG. 2. (Color online) yz-plane projection of relaxed structure of Mn-dimer supported on the CuN obtained by using LSDA method. Yellow, blue and red spheres correspond to Cu, N, and Mn atoms, respectively. Green arrows denote the directions of the atomic magnetic moments.

II. METHODS OF INVESTIGATION

A. DFT calculation details

We have used two complementary approaches to investigate the electronic structure and magnetic properties of Mn nanochains on the CuN surface.

(i) First-principles total energy and force calculations were carried out using the projected augmented-wave (PAW) method[11] as implemented in the Vienna *ab initio* simulation package (VASP).[12–14] Exchange and correlation effects have been taken into account using the local spin-density approximation and the local-density approximation taking into account the on-site Coulomb interaction (LDA+U).[15] In our calculations we used an energy cutoff of 400 eV in the plane-wave basis construction and the energy convergence criteria of 10^{-4} eV. The crystal structure was optimized until the forces acting on atoms were less than 0.01 eV/Å. For the Brillouin-zone integration, a $(4\times4\times1)$ Monkhorst-Pack mesh[16] and Gaussian-smearing approach with $\sigma=0.2$ eV were used.

It is well known that the L(S)DA underestimates lattice constants of bulk transition metals.[17] In particular the LDA bulk fcc Cu lattice constant is 3.51 Å in contrast to experi-

TABLE I. Relaxed crystal data obtained by LSDA and LDA+U approximations. The values of $d_{12}(d_{23})$ and z are distances (in Å) between Mn atoms and z coordinates of Mn (N) atoms at the center (edge) of chain, respectively. α is angle of Mn-N-Mn bond. Zero level of z coordinate corresponds to the lowermost layer of Cu atoms.

	d_{12}	d_{23}	z_{Mn}	z_N (center)	z_N (edge)	α_{12}	α_{23}
Dimer[a]	3.61		7.32	7.22	6.30	174°	
Dimer[b]	3.78		7.43	7.11	6.22	161°	
Trimer[b]	3.71	7.42	7.10	6.5	5.93	143°	143°
Tetramer[b]	3.68	7.27	7.02	6.4	5.92	142°	133°

[a]LSDA calculation.
[b]LDA+U calculation.

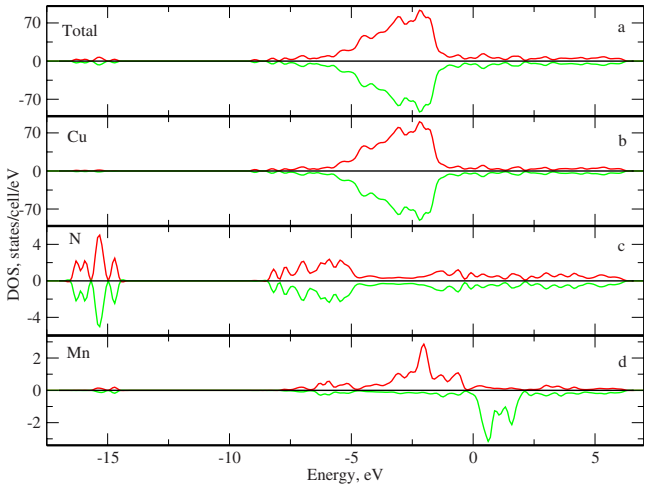

FIG. 3. (Color online) Total and partial density of states of Mn-dimer obtained from LSDA (PAW) calculations. (a) Total DOS, (b) Projected DOS onto Cu atoms, (c) Projected DOS onto N atoms, (d) Projected DOS onto Mn atom. The zero energy corresponds to the Fermi level.

mental value of 3.61 Å. For that purpose the lattice constant for initial fcc Cu lattice was chosen to be 3.61 Å in our calculations. The lowermost layer of Cu atoms has been fixed under relaxation. We have checked that the four layers CuN slab is enough to simulate CuN surface and subsequent increasing the number of layers does not significantly affect on the atomic structure, electronic, and magnetic properties. For instance, having compared results obtained with four and five layers slabs we have found that the difference in the resulting angles of Mn-N-Mn bond is less than 1°.

As for x-y extension of the supercells we used the different structures depending on the chain length (Fig. 1). Since CuN surface has almost insulating behavior the effective interactions between Mn-chains in the different cells are exponentially small. Therefore, we believe that the two free interatomic spacing for different Mn-chains shown in the Fig. 1 is enough to minimize the spurious supercell effects.

(ii) The second approach we used is the tight-binding linear-muffin-tin-orbital atomic sphere approximation (TB-LMTO-ASA) method[18] in terms of LSDA, LDA+U (Ref. 15) and spin-orbit coupling LDA+U+SO (Refs. 19 and 20) approaches. We would like to stress that we have used the same version of the LDA+U method in both PAW and TB-LMTO-ASA calculations. In TB-LMTO-ASA calculations we have used the relaxed atomic structures obtained with the PAW approach. The radii of atomic spheres have been set to r(Mn)=1.137 Å, r(Cu)=1.322 Å, and r(N)=0.793 Å. In order to fill the empty space of the unit cell required number of empty spheres was added.

B. Spin Hamiltonian approach

To analyze the magnetic properties of Mn nanochains on the CuN surface we use the following spin Hamiltonian:

$$H = H_{\mathrm{Heis}} + H_{\mathrm{DM}} + H_{\mathrm{anis}}, \tag{1}$$

where the Heisenberg[21] energy is

$$H_{\mathrm{Heis}} = \sum_{i<j} J_{ij} \hat{S}_i \hat{S}_j, \tag{2}$$

the Dzyaloshinskii-Moriya[22] energy is

$$H_{\mathrm{DM}} = \sum_{i<j} \vec{D}_{ij} [\hat{S}_i \times \hat{S}_j], \tag{3}$$

and the single-site anisotropy energy is

$$H_{\mathrm{anis}} = \sum_{i} \{A(\hat{S}_i^z)^2 + E[(\hat{S}_i^x)^2 - (\hat{S}_i^y)^2]\}. \tag{4}$$

The main task here is to define the isotropic and anisotropic exchange interaction parameters from first-principles calculations. The single-site anisotropy constants were recently calculated from the torque method[23] and resulting values of A and E are in reasonable agreement with the recent STM experiments.[4]

To calculate the isotropic exchange interactions J_{ij}, in Eq. (2) between magnetic moments of the Mn atoms we have used two different techniques. (i) Within so-called total energies difference method the isotropic exchange interaction is calculated by the difference of the total energies of simulated magnetic configurations. For instance, the spin Hamiltonian for Mn dimer is given by

$$H = J \hat{S}_1 \cdot \hat{S}_2. \tag{5}$$

The corresponding total energies of the ferromagnetic and antiferromagnetic configurations can be easily calculated for classical spins and the exchange interaction J can be expressed in the following form:

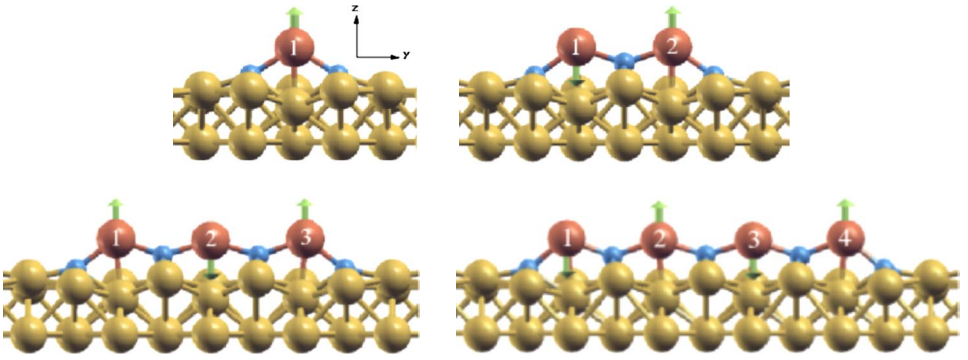

FIG. 4. (Color online) Relaxed structures of Mn chains on the CuN surface obtained from LDA+U calculations. The two topmost layers of the CuN slabs are presented. Yellow, blue, and red spheres correspond to Cu, N, and Mn atoms, respectively. Green arrows correspond to directions of magnetic moments of manganese atoms.

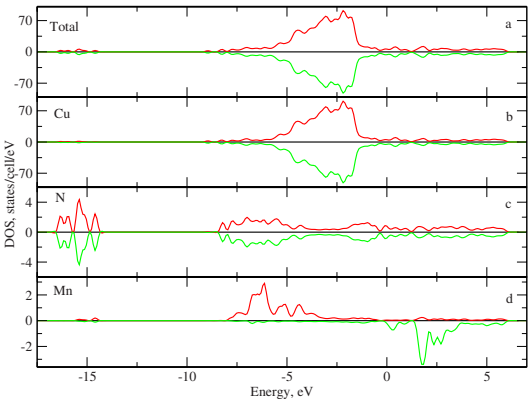

FIG. 5. (Color online) Total and partial density of states of Mn-dimer on CuN surface obtained from LDA+U calculations. (a) Total DOS, (b) projected DOS onto Cu atoms, (c) projected DOS onto N atoms, (d) projected DOS onto Mn atom. The zero energy corresponds to the Fermi level.

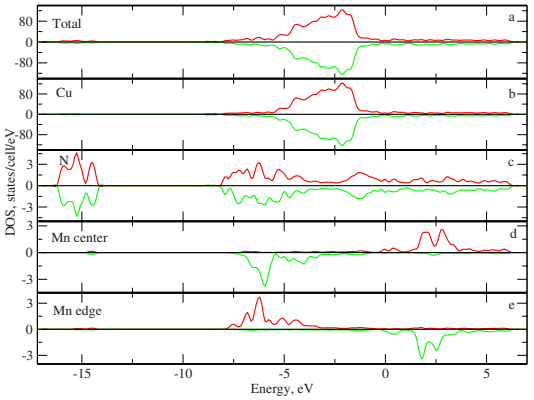

FIG. 6. (Color online) Total and partial density of states of Mn-trimer chain on CuN surface obtained from LDA+U calculations. (a) Total DOS, (b) projected DOS onto Cu atoms, (c) projected DOS onto N atoms, (d) projected DOS onto central Mn atom, (e) projected DOS onto edge Mn atom. The zero energy corresponds to the Fermi level.

$$J = \frac{E_{\mathrm{FM}} - E_{\mathrm{AFM}}}{2S^2}. \tag{6}$$

(ii) Within the TB-LMTO-ASA one can also calculate the isotropic exchange interactions between magnetic moments of Mn atoms ($S=\frac{5}{2}$) using the local force theorem and the Green's function technique[24–26]

$$J_{ij} = \frac{1}{2\pi S^2}\int_{-\infty}^{E_F} d\epsilon\, \mathrm{Im} \sum_{\substack{m,m' \\ m'',m'''}} (\Delta_i^{mm'} G_{ij\downarrow}^{m'm''} \Delta_j^{m''m'''} G_{ji\uparrow}^{m'''m}), \tag{7}$$

where m, m', m'', and m''' are magnetic quantum numbers and the on-site potential $\Delta_i^{mm'} = H_{ii\uparrow}^{mm'} - H_{ii\downarrow}^{mm'}$. The Green's function is calculated in the following way:

$$G_{ij\sigma}^{mm'}(\epsilon) = \sum_{\mathbf{k},n} \frac{c_{i\sigma}^{mn}(\mathbf{k}) c_{j\sigma}^{m'n*}(\mathbf{k})}{\epsilon - E_\sigma^n(\mathbf{k})}. \tag{8}$$

Here $c_{i\sigma}^{mn}$ is a component of the nth eigenstate, E_σ^n is the corresponding eigenvalue and $\mathbf{k}$ is quasimomentum in the first Brillouin zone.

Taking into account spin-orbit coupling the Dzyaloshinskii-Moriya interaction, Eq. (3) can be calculated using the second variation in the total energy over small deviations of magnetic moments from a collinear ground state:[25,27]

$$\begin{aligned} D_{ij}^z = -\frac{1}{2\pi S^2} Re \int_{-\infty}^{E_F} d\epsilon \sum_k (&\Delta_i G_{ik}^{\downarrow} H_{k\downarrow\downarrow}^{\mathrm{so}} G_{kj}^{\downarrow} \Delta_j G_{ji}^{\uparrow} \\ &- \Delta_i G_{ik}^{\uparrow} H_{k\uparrow\uparrow}^{\mathrm{so}} G_{kj}^{\uparrow} \Delta_j G_{ji}^{\downarrow} + \Delta_i G_{ij}^{\downarrow} \Delta_j G_{jk}^{\uparrow} H_{k\uparrow\uparrow}^{\mathrm{so}} G_{ki}^{\uparrow} \\ &- \Delta_i G_{ij}^{\uparrow} \Delta_j G_{jk}^{\downarrow} H_{k\downarrow\downarrow}^{\mathrm{so}} G_{ki}^{\downarrow}), \end{aligned} \tag{9}$$

where $H_k^{\mathrm{so}} = \lambda_k \vec{L}\vec{S}$ and λ_k is spin-orbit coupling constant for site k. We have used the value $\lambda = 47$ meV calculated by using the LDA+U+SO approach.[20] Here we present only the z component of the Dzyaloshinskii-Moriya vector. The x and y components can be obtained from the z ones by rotation of the coordinate system.

III. RESULTS

A. LSDA results

We have performed the LSDA calculations of an antiferromagnetic Mn-dimer supported on the CuN surface. Figure 2 shows the relaxed structure of the Mn-dimer obtained using the PAW method. The information about relaxed dimer structure is presented in Table I. One can see that Mn-N-Mn bond angle of 174° is close to 180° that corresponds to the maximum of superexchange interaction between 3d atoms.

The total and partial densities of states obtained by using the PAW approach are presented in Fig. 3. The valence band contains low and high energy parts separated by 6 eV. The low energy states located around −15 eV have mainly N origin. In the high energy part (between −7 and 5 eV) all states are highly mixed.

The calculated TB-LMTO-ASA and PAW values of the magnetic moments of Mn atoms are $3.78\mu_B$ and $3.34\mu_B$, respectively. These values are substantially smaller than experimentally observed spin-$\frac{5}{2}$. The calculated exchange parameter J_{ij} within the Green's function approach, Eq. (7) is 20.4 meV, whereas total energies difference method value, Eq. (6) is 24.8 meV. These values are at least three times larger than that extracted from experiment.[4] Thus, one can see that the main electronic and magnetic properties of the Mn-dimer cannot be correctly reproduced within the LSDA approach.

B. LDA+U results

The results of Sec. III A have demonstrated the drawbacks of the LSDA approach to describe the magnetic properties of the Mn-dimer on the CuN surface. It is a well-known problem of the local-density approximation in case of transition-metal compounds.[15] To overcome this problem we

TABLE II. Values of magnetic moments of Mn atoms (in μ_B) calculated using LMTO (PAW) method.

n	M_{edge}	M_{center}
1	4.70 (4.69)	
2	4.32 (4.37)	
3	4.34 (4.42)	4.37 (4.32)
4	4.41 (4.39)	4.45 (4.35)

have used the LDA+U approximation that takes into account the Coulomb correlations of localized states neglected in LDA. The on-site Coulomb interaction U and the intra-atomic exchange interaction J_H of the manganese atoms are 5.88 and 0.88 eV, respectively. We have chosen these values for two reasons. (i) The effective Coulomb interaction $U_{\text{eff}} = U - J_H$ agrees with that calculated in Ref. 6. (ii) As we will show below the isotropic exchange interactions calculated using the LDA+U approach are in good agreement with those extracted from the STM experiment.[4]

The relaxed structures of the single, dimer, trimer, and tetramer systems calculated within the PAW method are shown in Fig. 4. We summarize information about relaxed atomic structures in Table I. Let us analyze difference between CuN surface systems with and without Mn atoms. Placing Mn atoms on top of Cu atom in the CuN surface causes a substantial rearrangement of upper layer atoms of the CuN substrate. This rearrangement concerns the N atoms and, in contrast to bare CuN, for the system with Mn nanochains they are significantly shifted from the top layer. This fact agrees with results of the recent GGA calculations.[5] The calculated LDA+U angle of the Mn-N-Mn bond equals to 161°. The N atoms at the edges of chains also have some displacement from the plane in z direction, but to a smaller extent than N atoms situated inside the chain.

From a geometrical point of view the important difference between results of LSDA and LDA+U calculations is the angle of Mn-N-Mn bond. Let us analyze this fact within the framework of hopping integrals. For simplicity, we assume that there is the only strong hopping parameter between orbitals of two 3d atoms. The hopping integral t_{ij} is proportional to cos α, where α is an angle of metal-ligand-metal bond. The isotropic exchange interaction between transition metal atoms in the atomic limit of Hubbard model can be expressed as $J_{ij} = \frac{4t_{ij}^2}{U}$, here U is on-site Coulomb integral. One can see that both the hopping integral and the isotropic exchange interaction are strongly suppressed within LDA+U approach.

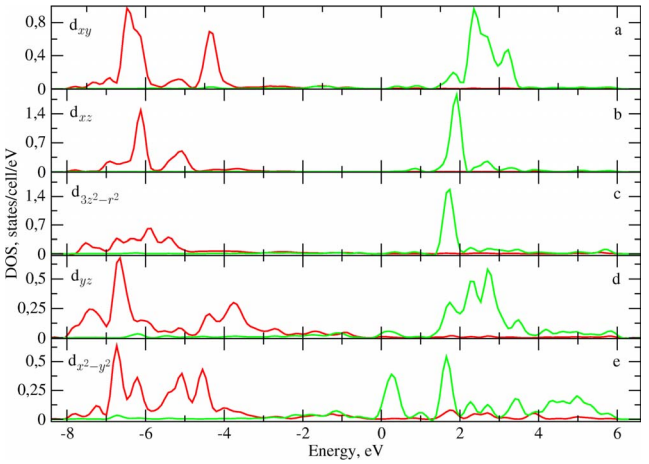

FIG. 7. (Color online) Partial densities of 3d states of manganese atom obtained from LDA+U calculations of Mn dimer. The red and green solid lines correspond to spin-up and spin-down states, respectively. The zero energy corresponds to the Fermi level.

TABLE III. Values of exchange interactions J_{ij} (in meV) between magnetic moments of Mn atoms calculated using the Green's function method (TB-LMTO-ASA). Values obtained using total energies difference method (PAW) are given in parenthesis.

n	J_{12}	J_{13}	J_{23}	J_{34}	J_{24}
2	6.5 (6.8)				
3	5.0 (5.1)	−0.5 (−0.6)	5.0 (5.1)		
4	6.2 (6.0)	−0.5 (−1.0)	5.6 (6.4)	6.2 (6.0)	−0.5 (−1.0)

The total and partial densities of states of the dimer and trimer systems obtained by using the LDA+U approximation are presented in Figs. 5 and 6, respectively. The calculated value of the magnetic moments is listed in Table II. One can see that the values of magnetic moments of Mn atoms vary from 4.7μ_B (single atom) to 4.3μ_B (dimer). A similar trend was observed in previous calculations. The obtained values are in better agreement with experimentally determined value of $S = \frac{5}{2}$.

Let us qualitatively discuss the single-site anisotropy of the Mn-dimer using LDA+U partial densities of states shown in Fig. 7. The main feature of the DOS is a broadening of the density of states of the $d_{x^2-y^2}$ orbital which strongly contributes to states near the Fermi level. According to the Bruno analysis (Ref. 28) the magnetic anisotropy energy is proportional to the difference of orbital moments and therefore connected with orbital-polarization above and below the Fermi level. Consequently, the main contribution to the anisotropy is provided by 3d states of x^2-y^2 symmetry. As we will show below the easy axis of Mn-dimer system is along z direction which related to the $\langle x^2-y^2|L|xy\rangle$ matrix element of the orbital moment operator. We have also found that the LSDA density of states are qualitatively similar to LDA+U results in the vicinity of the Fermi level.

C. Isotropic exchange interaction

The next step of our investigation is determination of the Heisenberg exchange interaction parameters in Eq. (2). The

TABLE IV. Energies of first-excited states (in meV) of the Heisenberg model obtained by using ALPS code.

n	E^{exp}	$E^{\text{calc}}_{\text{LMTO}}$	$E^{\text{calc}}_{\text{PAW}}$
2	6.4	6.5	6.8
3	16.0	15.0	15.8
4	2.9	3.2	3.2

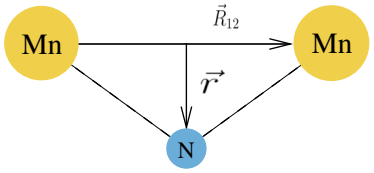

FIG. 8. (Color online) Schematic representation of displacement of the ligand atom.

magnetic couplings between Mn atoms calculated using the Green's function technique [Eq. (7)] and the total energies difference method [Eq. (6)] are presented in Table III. One can see that the obtained values of the dimer interaction are in good agreement with the experimental result of 6.4 meV. The value of the isotropic exchange integral between nearest Mn atoms in the trimer is smaller than that in the dimer system. In addition, there is a small ferromagnetic coupling between edge Mn atoms. As we will show below this coupling plays an important role for accurate description of the experimental spectrum.

In the case of the Mn-tetramer there is a difference between exchange integrals J_{12} and J_{23}. The PAW coupling between central atoms of the chain is smaller than that between edge atoms. This result probably corresponds to oscillations of the exchange interaction parameter depending on chain length. It is important to identify the source of these strong oscillations (see Mn_3 results in Table III) of nearest-neighbor exchange interactions in Mn_n nanochains. Such analysis is left for future investigation.

Using the full diagonalization subroutine of the ALPS library[29,30] we have calculated spin excitation spectra. The energies of first-excited states are presented in Table IV. Despite of the fact that the J_{12} of the trimer has smaller value than in the dimer case, a weak ferromagnetic J_{13} interaction between edge atoms compensates this difference. It gives us opportunity to reproduce experimentally observed excitation energies with a good accuracy.

D. Dzyaloshinskii-Moriya interaction

From a crystal symmetry point of view there is no inversion center at the point bisecting the straight line between Mn atoms of the investigated nanosystems. Therefore, in accordance with Moriya's rules[22] a Dzyaloshinskii-Moriya coupling exists. Let us first perform a simple geometrical analysis of the symmetry of the Dzyaloshinskii-Moriya vector. There are two sources of the inversion symmetry breaking in the investigated systems. (i) The first one is a substrate surface. Based on the fact that results of the previous investigations of metallic nanochains on nonmagnetic 3*d* surfaces have no sign of noncollinearity, one can conclude that the surface gives a negligibly small contribution to the anisotropic exchange interaction. (ii) More importantly, the second source of the inversion symmetry breaking is a vertical displacement of N atom. The Dzyaloshinskii-Moriya vector, $\vec{D}_{12}$ between Mn atoms is proportional to $[\vec{r}\times\vec{R}_{12}]$,[31] where $\vec{R}_{12}$ is a unit vector along the line connecting the magnetic ions and $\vec{r}$ is a shift of the ligand atom from this line (Fig. 8). One can see that in our case $\vec{r}$ and $\vec{R}_{12}$ have z and y components, respectively. Therefore, the direction of the Dzyaloshinskii-Moriya vector is x axis.

TABLE V. Values of the x component of the Dzyaloshinskii-Moriya interactions $\vec{D}_{ij}$ (in meV) between magnetic moments of Mn atoms calculated by using the Green's function method [Eq. (9)] within LDA+U approach.

n	D^x_{12}	D^x_{23}	D^x_{34}
2	0.015		
3	0.013	0.013	
4	0.01	0.008	0.01

TABLE VI. Values of canting angles and y components of the net magnetic moments (in μ_B) obtained by minimizing of the classical spin Hamiltonian [Eq. (1)].

n	Angle	M^y_{model}
2	α=0.07°	0.008
3	α=0.13°, β=0.03°, γ=0.07°	0.002
4	α=0.11° β=0.03°	0.012

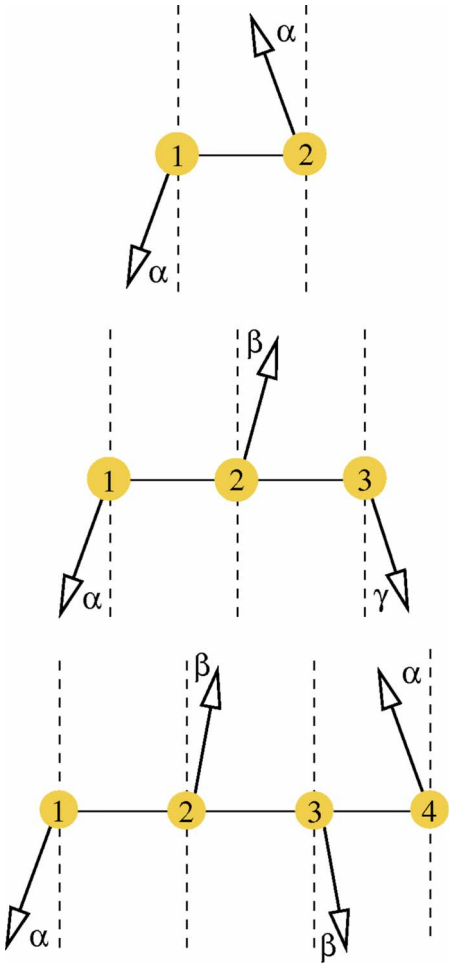

FIG. 9. (Color online) Schematic representation of spin canting of dimer, trimer, and tetramer systems.

TABLE VII. Calculated magnitude and orientation of the spin and orbital moments in a Mn dimer on the CuN surface.

Atom	Spin moment	Orbital moment
1	$4.3\times(0.0,0.004,-0.999)$	$0.14\times(0.0,-0.53,0.85)$
2	$4.3\times(0.0,0.004,0.999)$	$0.14\times(0.0,0.53,0.85)$

The calculated anisotropic exchange interactions, Eq. (9) are presented in Table V. For all systems under consideration the Dzyaloshinskii-Moriya vector lies along x axis (perpendicular to the Mn chain and parallel to the CuN surface). Therefore, if all spins lie in the yz plane, the canting exists and there is weak ferromagnetism. The ratio between Dzyaloshinskii-Moriya and isotropic exchange interactions, $\frac{|\vec{D}_{12}|}{J_{12}}=0.002$ is of the same order of magnitude as in case of well-known antiferromagnets Fe_2O_3 and La_2CuO_4 with weak ferromagnetism.

We minimized the classical spin Hamiltonian [Eq. (1)] with first-principles exchange parameters in respect to the directions of the individual spins. The obtained values of the canting angles and net magnetic moments of the Mn nanochains are presented in Table VI and Fig. 9. One can see that the net magnetic moment increases with length of the nanochain. Therefore one can expect that the weak ferromagnetism can be experimentally observed for long nanochains.

In order to test the reliability of the weak ferromagnetism results for the dimer we have performed the LDA+U+SO calculations in the framework of PAW scheme. The size and the direction of the spin and orbitals moments extracted from the equilibrium state are shown in Table VII. One can see that there are spin and orbital contributions of the same order to the total magnetic moment canting. Another interesting point is that the z components of the orbital magnetic moments have the same sign. It means that the magnitudes of the total magnetic moments are slightly different.

The resulting canted ground state is in good agreement with experimental observations[6] where the easy axis of a system with single Mn atom on the CuN surface is z axis. The spin canting angle of 0.21° obtained by using the LDA+U+SO calculations corresponds to the following Dzyaloshinskii-Moriya interactions $D^x_{ij}=J_{ij}\tan(\pi-2\alpha)=0.047$ meV. The obtained values of the model canting angles for the dimer (Table VI) are about three times smaller than those obtained in our first-principles LDA+U+SO calculations. This can be related with spherical approximations for the Green's function technique for estimating the Dzyaloshinskii-Moriya parameters [Eq. (9)].

Clearly, the ultimate test of our results will to compare them with experiment. Unfortunately, at the moment there are no magnetization measurements on Mn nanochains on the CuN surface. In Sec. IV we will show that some aspects of an experimental spectrum[4] can be explained by using a quantum spin Hamiltonian.

IV. ZERO-FIELD SPLITTING

To explain experimentally observed different zero-field energy of $m=\pm1$ and $m=0$ excited states[4] we use the following quantum spin Hamiltonian:

TABLE VIII. Matrix elements of the Heisenberg Hamiltonian Eq. (11).

	$\|\uparrow,\uparrow\rangle$	$\|\downarrow,\downarrow\rangle$	$\|\uparrow,\downarrow\rangle$	$\|\downarrow,\uparrow\rangle$
$\|\uparrow,\uparrow\rangle$	$\frac{J}{4}$	0	$\frac{iD^x_{12}}{4}$	$-\frac{iD^x_{12}}{4}$
$\|\downarrow,\downarrow\rangle$	0	$\frac{J}{4}$	$-\frac{iD^x_{12}}{4}$	$\frac{iD^x_{12}}{4}$
$\|\uparrow,\downarrow\rangle$	$-\frac{iD^x_{12}}{4}$	$\frac{iD^x_{12}}{4}$	$-\frac{J}{4}$	$\frac{J}{2}$
$\|\downarrow,\uparrow\rangle$	$\frac{iD^x_{12}}{4}$	$-\frac{iD^x_{12}}{4}$	$\frac{J}{2}$	$-\frac{J}{4}$

$$\hat{H}=J\hat{S}_1\hat{S}_2+\vec{D}_{12}[\hat{S}_1\times\hat{S}_2]+\sum_i\{A_i(\hat{S}^z_i)^2+E_i[(\hat{S}^x_i)^2-(\hat{S}^y_i)^2]\}, \tag{10}$$

where A_i and E_i are axial and transversal contributions to the single-site anisotropy.[4]

For simplicity, let us first consider the case of $S=\frac{1}{2}$ and $\vec{D}_{12}=(D^x_{12};0;0)$. Since the single-site anisotropy vanishes for $S=\frac{1}{2}$ one can rewrite Eq. (10) in the following form:

$$\hat{H}=J(\hat{S}^x_1\hat{S}^x_2+\hat{S}^y_1\hat{S}^y_2+\hat{S}^z_1\hat{S}^z_2)+D^x_{12}(\hat{S}^y_1\hat{S}^z_2-\hat{S}^z_1\hat{S}^y_2). \tag{11}$$

The basis functions for this Hamiltonian can be written as follows,

$$|\uparrow,\uparrow\rangle \quad |\downarrow,\downarrow\rangle \quad |\uparrow,\downarrow\rangle \quad |\downarrow,\uparrow\rangle. \tag{12}$$

Using well-known rules for spin operators,

$$\hat{S}^x|\uparrow\rangle=\frac{1}{2}|\downarrow\rangle \quad \hat{S}^y|\uparrow\rangle=\frac{i}{2}|\downarrow\rangle \quad \hat{S}^z|\uparrow\rangle=\frac{1}{2}|\uparrow\rangle$$

$$\hat{S}^x|\downarrow\rangle=\frac{1}{2}|\uparrow\rangle \quad \hat{S}^y|\downarrow\rangle=-\frac{i}{2}|\uparrow\rangle \quad \hat{S}^z|\downarrow\rangle=-\frac{1}{2}|\downarrow\rangle,$$

one can define the matrix elements of this Hamiltonian presented in Table VIII. The eigenvalues of this matrix are given by

$$E^{\pm}_T=\frac{J}{4},$$

$$E^0_T=-\frac{J}{4}+\frac{\sqrt{J^2+4(D^x_{12})^2}}{2},$$

$$E_S=-\frac{J}{4}-\frac{\sqrt{J^2+4(D^x_{12})^2}}{2}.$$

One can see that the energies of $m=0$ and $m=\pm1$ triplet states are different. Therefore, one might expect that the anisotropic exchange interaction helps us to explain the similar difference in the experimental spectra for the Mn dimer on the CuN surface.

Since in the case of $S=5/2$ the situation is more complicated, we have numerically calculated the excitation spectra by means of the ALPS library[29,30] using the single-site anisotropy estimated in Ref. 6 and the obtained exchange interactions. These results are presented in Table IX. One can see

TABLE IX. The energies of the three lowest excited states obtained by diagonalizing Eq. (11) with $J=6.5$ meV, $D=0.015$ meV, $A=-0.039$ meV and $E=0.007$ meV.

	E_1	E_2	E_3
This work	6.33	6.54	6.63
Expt. (Ref. 6)	5.96 ± 0.05	5.83 ± 0.05	5.83 ± 0.05

that the calculated first-excited states have different energies in the zero magnetic field. This is a result of the single-site anisotropy terms of the spin Hamiltonian [Eq. (10)]. According to the experiment[6] the zero-field energies of the first-excited states are 5.96 ± 0.05 and 5.83 ± 0.05 meV for $m=0$ and $m=\pm1$, respectively, and correspond to $\Delta E^{\text{exp}}=0.13\pm0.05$ meV. We can compare this value with the calculated splitting between maximum and minimum energies of the first-excited states, $\Delta E^{\text{calc}}=E_3-E_1=0.3$ meV (Table IX). Taking into account some ambiguities in determination of the experimental splitting we conclude that there is good agreement between theoretical and experimental results.

Using the spin Hamiltonian with the Dzyaloshiskii-Moriya interaction estimated from the LDA+U+SO calculations ($D_{ij}^{x}=0.047$ meV) we obtained the same splitting picture. Therefore, in quantum case there is a tiny effect of the Dzyaloshinskii-Moriya interaction on the excitation spectrum.

V. CONCLUSION

We have performed a first-principles investigation of the electronic and magnetic structures of Mn nanochains supported on the CuN surface. Based on the calculated isotropic and anisotropic exchange interactions we propose the antiferromagnetic ground state with weak ferromagnetism. It results from the atomic structure distortion that breaks the inversion symmetry between Mn atoms. The calculated values of the canting angles are of the same order as for classical antiferromagnets with weak ferromagnetism, Fe_2O_3 and La_2CuO_4. Using quantum spin Hamiltonian we have explained the experimentally observed different zero-field energies of $m=0$ and $m=\pm1$ states. Based on our results we suggest the noncollinear magnetic phenomenon for general surface nanosystems. For instance, we found significant spin-orbit canting effect in Co nanochain on a Pt surface.

ACKNOWLEDGMENTS

We would like to thank F. Mila, M. Troyer, M. Sigrist, I.V. Solovyev, and F. Lechermann for helpful discussions. The hospitality of the Institute of Theoretical Physics of Hamburg University is gratefully acknowledged. This work is supported by DFG Grant No. SFB 668-A3 (Germany), INTAS Young Scientist Fellowship Program Ref. No. 04-83-3230, Russian Foundation for Basic Research Grants No. RFFI 07-02-00041 and No. RFFI 06-02-81017, the grant program of President of Russian Federation Grant No. MK-1041.2007.2, Intel Scholarship Grant and the scientific program "Development of scientific potential of universities" Grant No. 2.1.1/779. The calculations were performed using the facilities of the "University Center of Parallel Computing" of USTU-UPI and Gonzales cluster at ETH-Zurich.

[1] Y. Zhang, N. Kohler, and M. Zhang, Biomaterials **23**, 1553 (2002).
[2] T. Neuberger, B. Schopf, H. Hofmann, M. Hofmann, and B. von Rechenberg, J. Magn. Magn. Mater. **293**, 483 (2005).
[3] D. Bajalan and J. A. Aziz, Progress In Electromagnetics Research Symposium Online, 2, 461 2006.
[4] C. F. Hirjibehedin, C. P. Lutz, and A. J. Heinrich, Science **312**, 1021 (2006).
[5] C.-Y. Lin, B. Jones, and A. Heinrich, APS March Meeting, 2006.
[6] C. F. Hirjibehedin, C.-Y. Lin, A. F. Otte, M. Ternes, C. P. Lutz, B. A. Jones, and A. J. Heinrich, Science **317**, 1199 (2007).
[7] H. J. Gotsis, N. Kioussis, and D. A. Papaconstantopoulos, Phys. Rev. B **73**, 014436 (2006).
[8] A. Bergman, L. Nordstrom, A. Burlamaqui Klautau, S. Frota-Pessoa, and O. Eriksson, Phys. Rev. B **75**, 224425 (2007); **73**, 174434 (2006).
[9] S. Lounis, P. Mavropoulos, R. Zeller, P. H. Dederichs, and S. Blügel, Phys. Rev. B **75**, 174436 (2007).
[10] M. Bode, M. Heide, K. von Bergmann, P. Ferriani, S. Heinze, G. Bihlmayer, A. Kubetzka, O. Pietzsch, S. Blügel, and R. Wiesendanger, Nature (London) **447**, 190 (2007).
[11] P. E. Blöchl, Phys. Rev. B **50**, 17953 (1994).
[12] http://cms.mpi.univie.ac.at/vasp/.
[13] G. Kresse and D. Joubert, Phys. Rev. B **59**, 1758 (1999).
[14] J. Hafner, J. Comput. Chem. **29**, 2044 (2008).
[15] V. I. Anisimov, F. Aryasetiawan, and A. I. Lichtenstein, J. Phys.: Condens. Matter **9**, 767 (1997).
[16] H. J. Monkhorst and J. D. Pack, Phys. Rev. B **13**, 5188 (1976).
[17] S. Khmelevskyi, P. Mohn, J. Redinger, and M. Weinert, Phys. Rev. Lett. **94**, 146403 (2005).
[18] O. K. Andersen, Phys. Rev. B **12**, 3060 (1975).
[19] I. V. Solovyev, A. I. Liechtenstein, V. A. Gubanov, V. P. Antropov, and O. K. Andersen, Phys. Rev. B **43**, 14414 (1991).
[20] A. O. Shorikov, A. V. Lukoyanov, M. A. Korotin, and V. I. Anisimov, Phys. Rev. B **72**, 024458 (2005).
[21] W. Heisenberg, Z. Phys. **49**, 619 (1928).
[22] T. Moriya, Phys. Rev. **120**, 91 (1960).
[23] A. B. Shick, F. Máca, and A. I. Lichtenstein, arXiv:0810.3389 (unpublished).
[24] A. I. Liechtenstein, M. I. Katsnelson, V. P. Antropov, and V. A. Gubanov, J. Magn. Magn. Mater. **67**, 65 (1987).
[25] V. V. Mazurenko and V. I. Anisimov, Phys. Rev. B **71**, 184434 (2005).
[26] I. V. Solovyev, P. H. Dederichs, and I. Mertig, Phys. Rev. B **52**, 13419 (1995).
[27] I. Solovyev, N. Hamada, and K. Terakura, Phys. Rev. Lett. **76**, 4825 (1996).
[28] P. Bruno, Phys. Rev. B **39**, 865 (1989).

[29] F. Alet, S. Wessel, and M. Troyer, Phys. Rev. E **71**, 036706 (2005).

[30] F. Alet *et al.*, J. Phys. Soc. Jpn. **74**, 30 (2005); A. F. Albuquerque *et al.*, J. Magn. Magn. Mater. **310**, 1187 (2007); M. Troyer, B. Ammon, and E. Heeb, Lect. Notes Comput. Sci. **1505**, 191 (1998).

[31] S.-W. Cheong and M. Mostovoy, Nature Mater. **6**, 13 (2007).